Available online at www.sciencedirect.com
SCIENCE DIRECT®
Composites: Part B 35 (2004) 235–243
composites Part B: engineering
www.elsevier.com/locate/compositesb

On styrene–butadiene–styrene–barium ferrite nanocomposites

M. Chipara[a,*], D. Hui[b], J. Sankar[c], D. Leslie-Pelecky[d], A. Bender[d], L. Yue[d], R. Skomski[d], D.J. Sellmyer[d]

[a]*Indiana University Cyclotron Facility, 2401 Milo B Sampson Lane, Bloomington, IN 47408, USA*
[b]*Department of Mechanical Engineering, University of New Orleans, Lakefront, New Orleans, LA 70148, USA*
[c]*North Carolina A and T state University, Department of Mechanical Engineering, Greensboro, NC 27411, USA*
[d]*University of Nebraska, Department of Physics and Astronomy, Lincoln, NE 68508, USA*

Received 1 March 2003; revised 26 March 2003; accepted 15 April 2003

Abstract

Magnetic investigations on a nanocomposite material obtained by spinning solutions of styrene–butadiene–styrene block copolymer containing barium ferrite nanoparticles onto Si wafers are reported. The effect of the spinning frequency on the magnetic features is discussed. It is observed that the magnetization at saturation is decreased as the spinning frequency is increased as the centrifuge force removes the magnetic nanoparticles from the solution. This is supported by the derivative of the hysteresis loops, which show two components, one with a high coercive field and another with a small coercive field. Increasing the spinning frequency increases the weight of the low coercive field component. The anisotropy in the distribution of magnetic nanoparticles, triggered eventually by the self-assembly capabilities of the matrix, is revealed by the difference between the coercive field in parallel and perpendicular configuration. It is noticed that increasing the spinning frequency enhances this difference. The effect of annealing the nanocomposite films is discussed.

Keywords: Magnetization; Annealing; Block coplymer; Nanoparticle

1. Introduction

The preferential distribution of nanoparticles of various functionalities within block copolymers represents a future nano technology that would result in new composite materials with a wide range of potential applications. The controlled dispersion of magnetic nanometer sized particles into self-organized matrices will provide a cheap and efficient way to ultra high-density magnetic recording media. This contribution is focused on such applications.

1.1. Magnetic properties of nanoparticles

Mesoscopic magnetism attracted much interest triggered by novel magnetic behavior encountered in magnetic nano particles as well as by large potential applications. The magnetization of a macroscopic sample result from the minimum of its free energy. To reach this minimum, domains over which the individual moments are essentially pointing in the same direction are spontaneously generated. By shrinking the size of the magnetic particle, a critical diameter D_C is eventually reached (see Fig. 1). This diameter is determined by the value of the magnetization at saturation, M_S, and by the exchange constant, A [6];

$$D_C \approx \frac{k_0}{M_S}\sqrt{\frac{A}{\mu_0}} \tag{1}$$

where μ is the magnetic susceptibility of the sample, and k_0 is a constant of the order of 10^1 [8]. Usually, the critical diameter is ranging between 10 and 100 nm [6]. For ferromagnetic particles smaller than D_C, the domain formation is no more energetically favored. Hence, these particles will be single domain particles and all individual magnetic moments of the particle will point in the same direction [6]. For most magnetic particles, the critical diameter for single domain magnetic particles is ranging from 10 to 100 nm.

Another critical size is reached shrinking further the size of magnetic particles. Below it, the nanoparticle becomes superparamagnetic, as the orientation of the total magnetic moment of the nanoparticle becomes unstable towards thermal fluctuations [2,3]. In such extremely small magnetic

* Corresponding author. Tel.: +1-812-855-6051; fax: +1-812-855-6645.
E-mail address: mchipara@iucf.indiana.edu (M. Chipara).

1359-8368/03/$ - see front matter © 2003 Elsevier Ltd. All rights reserved.
doi:10.1016/S1359-8368(03)00054-4

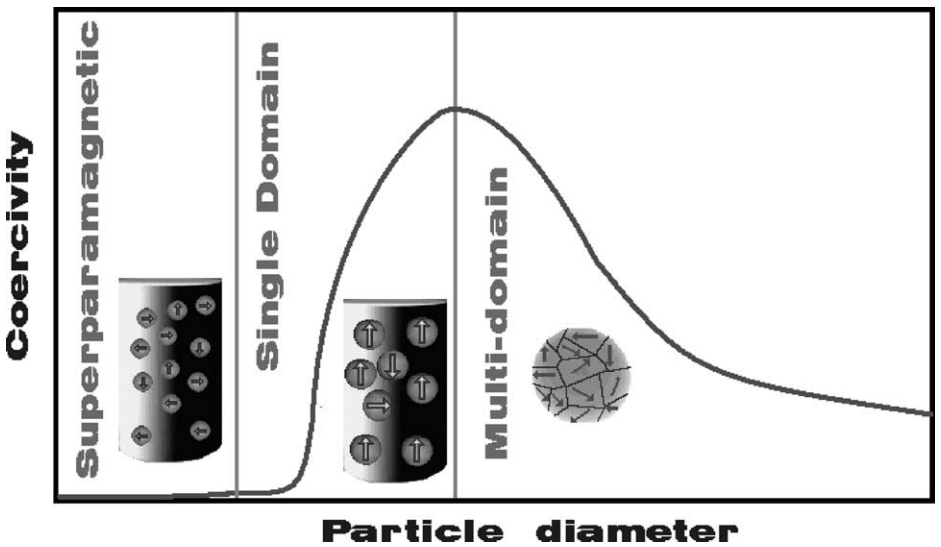

Fig. 1. The dependence of the coercive field on the particle size.

particles, it is possible to reach a situation in which the magnetic anisotropy is comparable to thermal fluctuations. This may be easily understand starting from the free energy of such a nanoparticles in an external magnetic field H, supposed to be applied along the OZ axis;

$$F = K_1 V \sin^2\theta - M_S H V \cos\theta \tag{2}$$

where K_1 is the uniaxial magnetocrystalline anisotropy, V the volume of the particle, μ the magnetic moment of the particle (equal to $M_S V$, where M_S is the magnetization at saturation) and θ the angle between the OZ axis and the magnetic moment of the particle. This simple system presents two extremes in the free energy, one corresponding to the magnetic moment aligned parallel to the external magnetic field ($\theta = 0$), of free energy $F_1 = M_S V H$, and the other characterized by an antiparallel orientation of the magnetic moment relative to the external magnetic field ($\theta = \pi$), with the free energy $F_2 = -M_S V H$. Due to thermal activation, the magnetic nanoparticle will oscillate between these states. This will require overcoming a potential barrier, of energy $F_{max} - F_1$. A simple calculation allows the estimation of F_{max};

$$F_{max} = K_1 V + \frac{M_S^2 H^2 V}{4K_1} \tag{3}$$

Hence the number of particles jumping over the barrier height per unit time is:

$$\nu = C\exp - \frac{(F_{max} \pm F_1)}{K_B T} = C\exp - \frac{K_1 V\left(1 + \dfrac{H}{2\dfrac{K_1}{M_s}}\right)^2}{K_B T} \tag{4}$$

where C is a constant. In the absence of the external magnetic field this probability becomes:

$$\nu_0 = C\exp - \frac{K_1 V}{K_B T} \tag{5}$$

If the particle is small enough and the time scale of the experiment T_{exp} is smaller than the reorientation time ν_0^{-1}, the experiment will average over the different orientations of the particles. Hence, in zero applied field the magnetization of the nanoparticles will be averaged out to zero, giving rise to superparamagnetism.

The temperature dependence of the superparamagnetic magnetization in an ideal superparamagnetic system consisting of weakly interacting particles is [3];

$$M_{SP} = \frac{\langle M_{nr}^2 V^2\rangle}{3K_B T\langle V\rangle} H_{eff} \tag{6}$$

M_{nr} is the non-relaxing magnetization of the particle, K_B the Boltzmann constant, $\langle V\rangle$ is the averaged value of particle's volume, and H_{eff} is the effective field seen the particle. This expression is valid for $M_{nr}^2 V H_{eff}/(K_B T) \ll 1$.

In magnetism, it is important to distinguish between the external magnetic field and the internal field that results from the competition between several contributions, which include the external magnetic field, the shape anisotropy, the magnetocrystalline anisotropy, and in certain cases higher order terms. In most cases, the experimental data are rather well fitted by a modified temperature dependence of the magnetization in the superparamagnetic state [3]:

$$M_{SP} = \frac{\langle M_{nr}^2 V^2\rangle}{K_B(T - T_{SP})\langle V\rangle} H_{eff} \tag{7}$$

where T_{SP} is the superparamagnetic temperature. Using a simplified Onsager model for an ensemble of non-spherical magnetic nanoparticles, the following expression for

the temperature dependence of susceptibility has been derived at high temperatures and small concentration of magnetic nanoparticles has been derived;

$$\chi_{SP} = \frac{C_{SP}}{T + T_{SP}} \quad C_{SP} = \frac{\langle M_{nr}^2 V^2 \rangle}{3K_B \langle V \rangle} \quad T_{SP}$$

$$= C_V(N_e - \frac{4\pi}{3})C_{SP} \tag{8}$$

where C_v is the volume concentration of magnetic nanoparticles and N_e is an average over the shape anisotropy of nanoparticles. The temperature dependence of the superparamagnetic susceptibility of γFe_2O_3 nanoparticles has been fitted with a slightly modified equation, that include the effect of the applied external magnetic field;

$$\chi_{SP} = \frac{C_{SP}}{T + aH + T_{SP}} \tag{9}$$

where a is a parameter related to the size and nature of nanoparticles [5].

In nanoparticles, surface effects are no more hidden by the bulk behavior, as the surface to bulk atoms ratio is significantly larger than in micron sized particles [2]. While the magnetic features of non interacting magnetic nanoparticles seems to be rather well described by actual models [7], the situation in which there is interactions among nanoparticles is still not properly understood and accurately described by existing formalisms [7].

In the case of a binary composite, the magnetization at saturation M_S^{COMP} is defined by;

$$M_S^{COMP} = w_1 M_S^{(1)} + w_2 M_S^{(2)} \tag{10}$$

where w_1 is the fraction of the magnetic filler in the composite, w_2 the fraction of the magnetic matrix in the composite, $M_S^{(1)}$ is the magnetization at saturation of the filler and $M_S^{(2)}$ the magnetization at saturation of the matrix [1].

The hexagonal barium ferrite is a potential material for future ultra high-density data storage. Such applications require magnetic nanoparticles with a diameter of 40–50 nm, a large aspect ratio, and high coerrcivity. Ba ferrite and substituted barium ferrites have the required properties, including a high coercivity (1750 to 2060 Oe) and excellent thermal stability [4]. The zero field magnetization at saturation M_S^0, and the anisotropy parameter, B, may be derived from the field dependence of the magnetization $M(H)$ [4];

$$M(H) = M_S^0[1 - \frac{A}{H} - \left(\frac{B}{H}\right)^2] + \chi_P H \tag{11}$$

where A is the inhomogeneity parameter and χ_P stands for a paramagnetic like correction to the magnetization (high field differential susceptibility [4]). For hexagonal ferrites, B is proportional to the anisotropy field H_A, which is dominated by the first order magnetocrystalline anisotropy, K_1 [4].

$$B \approx \frac{H_A}{\sqrt{15}} = \frac{2K_1}{\sqrt{15}M_S} \tag{12}$$

By introducing the shape anisotropy contribution for short ferromagnetic cylinders into the dependence (11), it will be noticed that the contribution of parameters A and χ_P is negligible [4]. The coercivity of barium ferrite, H_C, is controlled by the shape and magnetocrystalline anisotropies:

$$H_C = C\left(\frac{2K_1}{M_S} - NM_S\right) \tag{13}$$

where C is a constant and N reflects the shape anisotropy contribution. K_1 is rather an average anisotropy constant [4].

1.2. The self-assembly capabilities in block copolymers

The self-assembly capabilities of block copolymers reflect the spontaneous organization of macromolecular chain into intricate morphologies at nanometer scale, resulting from the minimum energy search. A simple block copolymer consists of two homopolymers linked together by chemical bond(s) into a new linear polymeric chain. The detailed of the architecture of macromolecular chains are controlled by the parameter χ^N, where χ represents the Flory Huggins interaction parameter and N the total degree of polymerization of the block copolymer. For a simple block copolymer build up of two homopolymers A and B, the interaction parameter α between these segments is extremely important [9];

$$\chi^N(T) = \alpha(T)(M_W^A \phi_A + M_W^B \phi_B) \tag{14}$$

where M_W^A is the weight average molecular weight of the homopolymer A, ϕ_A the specific volume of polymer A (in the block copolymer), M_W^B is the weight average molecular weight of the homopolymer B, ϕ_B the specific volume of polymer B. The temperature dependence of χ^N is dominated by the temperature dependence of the interaction parameter.

In the strong segregation limit, defined by the condition $\chi^N > 100$, the morphology of the block copolymer is essentially controlled by the volume fraction of the minority homopolymer, f_S, within the block copolymer. For small amounts of the homopolymer B (smaller than 20% in volume) the local morphology will consist of small spheres of polymer chains B in a polymer A sea (see the first morphology in Fig. 2). If the fraction of the polymer B is in the range 20–40% the morphology will consists of cylinders made of B chains in a sea of A chains. If the volume fraction of the component B is in the range 40–50%, the expected morphology will consist of alternating lamellae with segregated chains (see Fig. 2). Eventually, morphologies that are more complex may be observed. Increasing the volume fraction of the component B over 50% the roles of minority and majority chains are reversed (see Fig. 2). The interface between the two chains A and B, in the strong segregation limit is sharp (of the order of 2 nm).

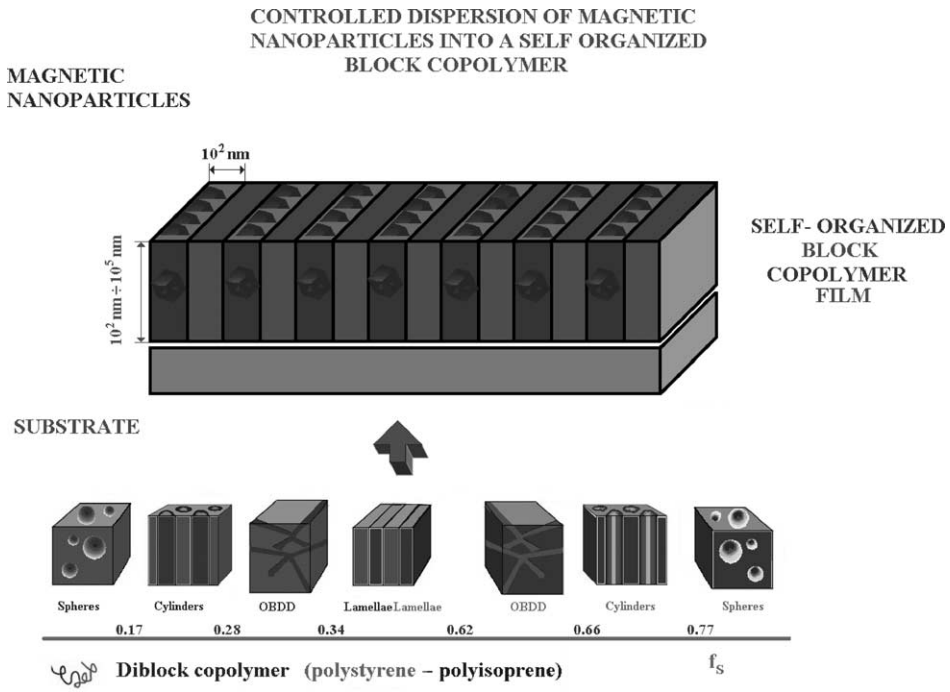

Fig. 2. Schematic of the future technology for ultra high magnetic data media, based on self-assembly capabilities.

1.3. Ultra high-density data storage media- an alternative future

Barium ferrite nanoparticles compete for the next ultra high-density magnetic media. A random distribution of magnetic nanoparticles on the surface of the magnetic media may require larger reading/write heads in order to compensate the local inhomogeneities in the nanoparticles surface distribution by averaging the magnetic signal. The preferential distribution of magnetic nanoparticles in a given phase of a block copolymer able to self organize would solved this problem without additional costs. A simple two-component block copolymer exhibits a wide range of morphologies- at nanometer range- depending on the volume fraction of components, f_S, (see for example Fig. 2). The lamella or cylinder like morphologies is the most promising morphologies for future magnetic media. Such a case is depicted in Fig. 2, where the track width is of the order of 100 nm and two adjacent tracks are separated by a non-magnetic lamella (cylinder). To survey the difficulties of such technologies, this paper is focused on the assessment of magnetic properties of nanometer size barium ferrite particles dispersed in a block copolymer (styrene–butadiene–styrene) that exhibits a lamella like morphology. The nanocomposite materials were obtained by spinning the solution polymer-magnetic nanoparticles. The effect of spinning frequency is studied.

2. Experimental methods

The nanocomposite has been obtained starting from poly(styrene-b-butadiene-b-styrene) (SBS) triblock copolymer from Aldrich Chemical, and barium dodecairon nonadecaoxide (barium ferrite- BaFe) powder from Aesar. The ferrite powder was milled to nanometer-sized particles by energetic ball milling. The size of BaFe nanoparticles was assessed from Wide Angle X-Ray Scattering measurements performed by using a Rigaku X-Ray Diffraction spectrometer. X-Ray diffraction spectra have been recorded after various milling times. The nanoparticles were introduced in a solution of 1% styrene–butadiene–styrene copolymer in chloroform, and sonicated in air at 50 °C for about 10 h. The weight of the barium ferrite–styrene–butadiene–styrene (BaFe–SBS) composite was measured daily by using a microbalance, in order to check for the complete removal of the solvent.

The magnetic properties of thin films of BaFe–SBS nanocomposites were tested by using an Alternating Gradient Force Magnetometer (AGFM). The hysteresis loops were measured in two configurations; the parallel one in which the external magnetic field is confined within the plane of the sample and the perpendicular configuration in which the external magnetic field is perpendicular to the plane of the sample.

Decreasing the amount of the magnetic component below 1% BaFe (weight), thin films of BaFe–SBS with a good transparency in visible that still exhibit a ferromagnetic behavior were obtained. Some samples have been annealed at 120 °C (above the highest glass transition temperature, which for polystyrene is about 100 °C) for 10 h and cooled extremely slow, in order to allow the reorganization of the block copolymer.

3. Experimental results

The size of nano particles was estimating from the line width of Wide Angle X-Ray Scattering spectra. The actual X-Ray diffractograms for various milling times are represented in Fig. 3. The inset represents the estimated dependence of the particle size on the milling time.

The hysteresis loops of BaFe–SBS nanocomposites obtained in the parallel configuration at various spinning frequencies are represented in Fig. 4. Quite unexpectedly, the parameters of the hysteresis loops are affected by the spinning frequency. The magnetization at saturation and anisotropy parameter B have been estimated from the dependence of the magnetization on the external magnetic field, for fields higher than the coercive field, by using the relationship (11).

Fig. 5 shows that increasing the spinning speed decreases the magnetization at saturation in both pristine and annealed samples. The dependence of the anisotropy parameter B and of the average magnetocrystalline anisotropy $K_1 \approx BM_S$ (see Eq. (12)), on the spinning frequency is illustrated in Fig. 6. The parameter BM_S decreases as the spinning frequency is increased in both pristine and annealed samples, for all orientations (parallel and perpendicular).

As the spinning frequency is raised, the coercive field decreases (see Fig. 7). To emphasize the complexity of the shape of hysteresis loops, the derivative of the negative branch of the hysteresis loop versus temperature is represented in Fig. 8. The appearance of a bimodal distribution is noticed.

4. Discussions

The actual study concerns barium ferrite nanoparticles dispersed in a polystyrene–polybutadiene–polystyrene block copolymer. As the polymeric matrix is diamagnetic ($M_S^{(2)} \approx 0$), the magnetization of the composite is controlled by the nanoparticles dispersed within the polymeric matrix. The reduced size of nanoparticles (about 15 nm) indicates that the particles are single domain. Hence, the external magnetic field will affect the orientation of individual spins. At such reduced sizes, a coherent or quasi-coherent magnetic nucleation processes are expected [8].

The decrease of the magnetization at saturation as the spinning frequency is increased (see Fig. 5) reflects the disappearance from the polymeric films of some nanoparticles. This is due to the large centrifuge forces that acting on nanoparticles during the spinning process. As the centrifuge force is proportional to the mass of particles, the bulkier particles will be removed firstly from the polymeric film. No significant annealing effects have been noticed. By increasing the spinning frequency the film thickness decreases. This may result in a decrease of the distance between magnetic nano particles. As the thickness of composite films deposited at frequencies larger than 10^3 rotations/minute is smaller

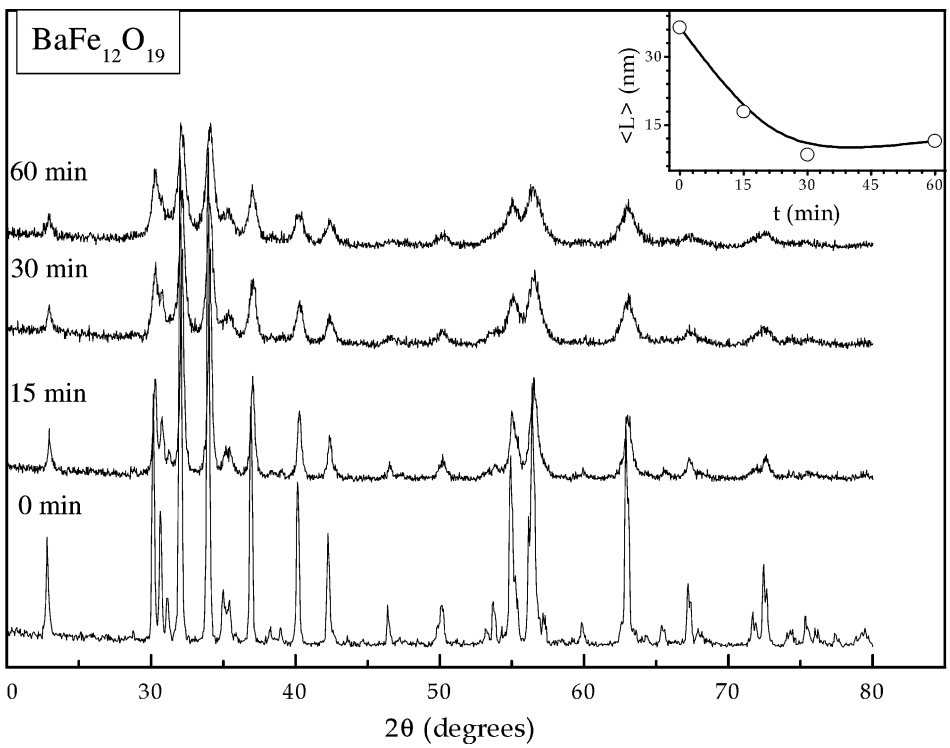

Fig. 3. The X-ray diffraction of BaFe at different milling times. The inset shows the dependence of the average length ⟨L⟩ on the milling time.

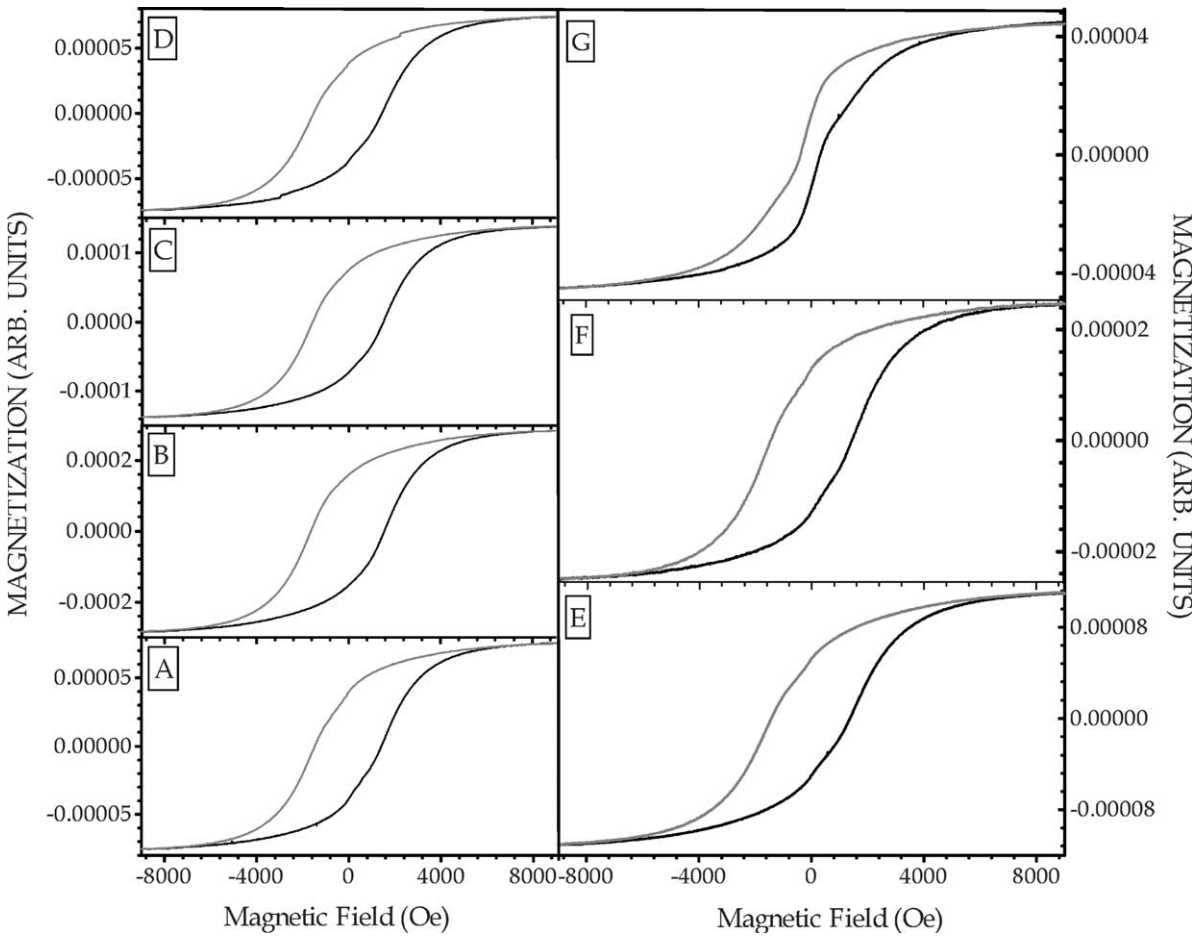

Fig. 4. The hysteresis loop in parallel orientation for pristine samples, at different spinning frequencies. A. 750 min^{-1}; B. 1000 min^{-1}; C. 2500 min^{-1}; D. 4000 min^{-1}; E. 5000 min^{-1}; F. 7000 min^{-1}; G. The hysteresis loop in the perpendicular orientation for a sample spanned at 7000 min^{-1}.

than 10^{-4} m, the decrease in the distance between barium ferrite nanoparticles would enhance the dipole–dipole interactions, leading to a decrease in the magnetization at saturation for the nano particles ensemble.

The gradual disappearance of 'bulk' magnetic nanoparticles is proved by the changes in the shape of the hysteresis loops as the spinning frequency is increased. The details of the hysteresis loops are better shown by the derivative of the negative branch (from the highest positive field to the highest negative field) versus the external magnetic field. As it is observed from Fig. 8, this derivative presents two peaks that would correspond to the inflection points of the hysteresis loop. The maxim (critical field) is expected to be located close to the coercive field of magnetic nanoparticles. As it is exhibited in Fig. 8, this peak is located near the coercive field while the other one is located at very small fields. This suggests that the size distribution of magnetic nanoparticles is rather large and that some superparamagnetic particles are present in the system. The relative increase of the amplitude of the maxim located at low magnetic field in comparison to the amplitude of the maxim located near the coercive field as the spinning frequency is increased is observed in Fig. 8. This result indicates that by increasing the spinning frequency, the fraction of small nano particles is increased and hence the relative weight of superparamagnetic particles is enhanced.

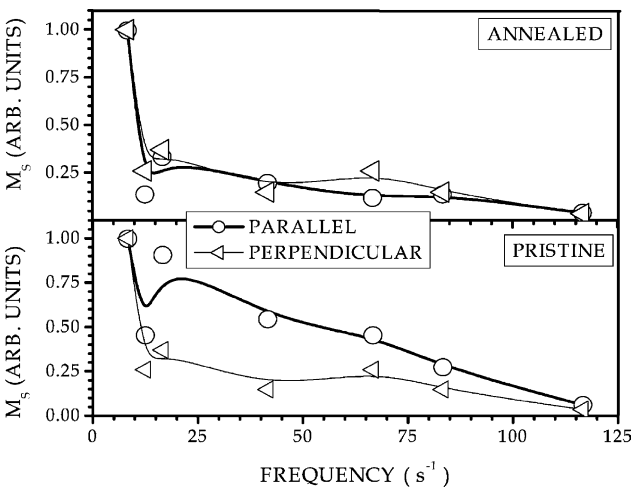

Fig. 5. The dependence of the magnetization at saturation on the spinning frequency for the annealed and pristine samples, respectively.

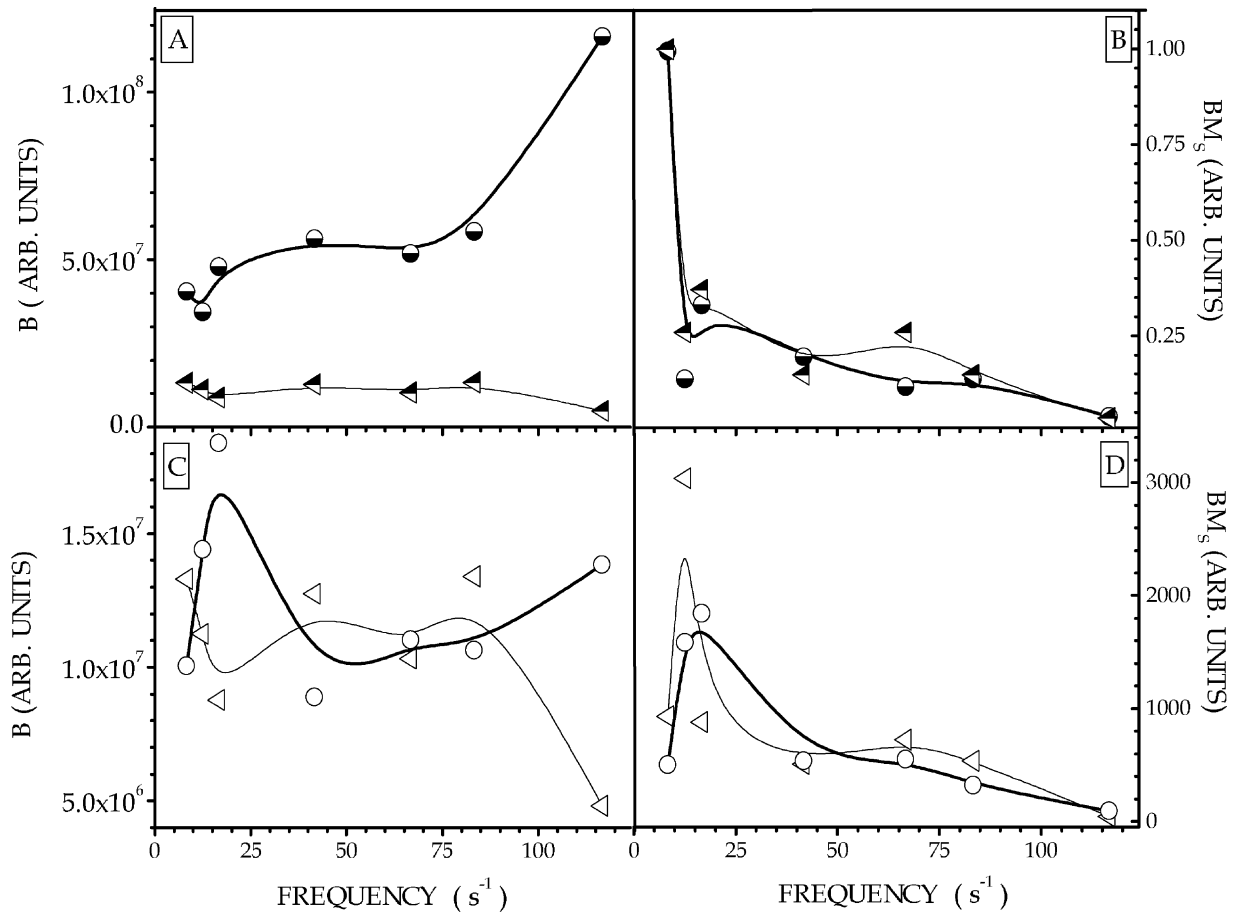

Fig. 6. A. The dependence of the parameter B on spinning frequency for the annealed sample. B. The dependence of the parameter BM_S on spinning frequency for the annealed sample. C. The dependence of the parameter B on spinning frequency for the pristine sample. D. The dependence of the parameter BM_S on spinning frequency for the pristine sample.

The dependence of the parameter B on the spinning frequency is also affected by the mass of magnetic nano particles retained within the film. Nevertheless, it is expected that the product BM_S would be independent on the number of nanoparticles, being proportional to the average anisotropy. As it is noticed from Fig. 5, as the spinning frequency is increased the value of the parameter BM_S is lowered in both pristine and annealed nano composites. This suggests the competition of two factors:

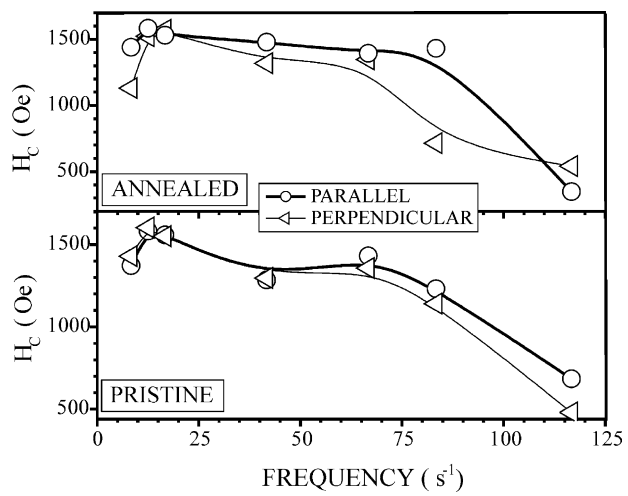

Fig. 7. The dependence of the derivative of the hysteresis loop versus magnetic field.

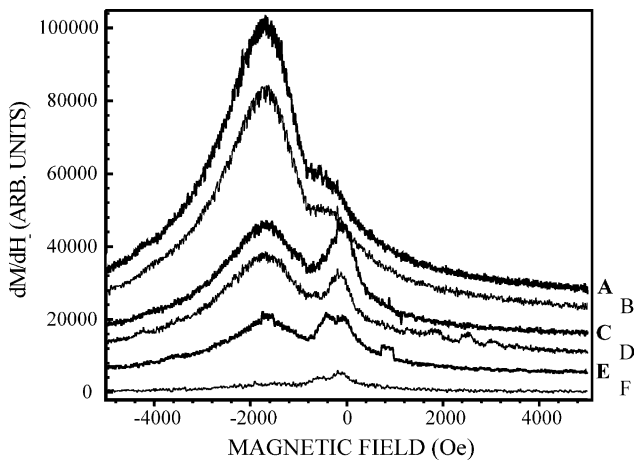

Fig. 8. The first derivative of the hysteresis loop (parallel configuration) versus the external magnetic field (descending branch) for films obtained at various spinning frequencies. A. 750 min^{-1}; B. 1000 min^{-1}; C. 2500 min^{-1}; D. 4000 min^{-1}; E. 5000 min^{-1}; F. 7000 min^{-1}.

1. Increasing the spinning frequency, the magnetocrystalline axes of magnetic particles are increasingly randomly distributed. A possible tendency of organization at small spinning frequency is possible.
2. It is important to recognize that the outcome of these measurements is not BM_S but rather an average value, over all nanoparticles present in the system. The small superparamagnetic particles would have almost no contribution to BM_S. Such a change in the size distribution of nanoparticles, due to the spinning frequency may also be responsible for the decrease of BM_S.

The analogy between the dependence of the magnetization at saturation and of BM_S on the spinning frequency suggests that this dependence is controlled by the magnetic nano particles concentration and the associated interactions between them.

In Fig. 7 it is observed that the coercive field decreases as the spinning frequency is increased. For curling nucleation modes in ellipsoids of revolution the nucleation field, H_N, is given by;

$$H_N = N_Z M_S - 2\frac{K_1}{M_S} - \frac{Cq^2}{M_S R^2} \tag{15}$$

where C is a constant, N_Z is the OZ component of the demagnetization tensor, q is another parameter and R is the ellipsoid semi axis in a direction perpendicular to the field direction (supposed along OZ). Assuming that $H_N \approx H_C$, it is observed that the homogeneous nucleation mode implies a coercive field independent on the size of the magnetic nanoparticles (see Eq. (14)), while the curling mode is characterized by a strong dependence of the coercive field on the particle size (see Eq. (15)). By decreasing the particle size, the coercive field value decreases. This is exactly the kind of dependence shown in Fig. 7.

There are also factors that would result in such a dependence of the coercive field on the spinning frequency. Higher spinning results in thinner films (the actual thickness at 5000 rotations/min was of the order of 0.1 μm). Hence, even if some magnetic particles are removed from the nanocomposite by centrifuge forces, the average distance between magnetic nanoparticles is in fact slightly reduced. Owing to the small distances among nanoparticles, dipole–dipole interactions between nanoparticles may decrease the magnetization at saturation, reducing the coercive field.

Increasing the spinning frequency, the difference between the parallel and perpendicular values of the coercive field is enhanced. This result may express either a preferential distribution of magnetic nanoparticles eventually related to the self-assembly features of the polymeric matrix or the fact that the number of next neighbors along a direction perpendicular to the plane is smaller that along a direction within the plane. Taking into account the effect of dipole–dipole interactions, the magnetization at saturation in plane would be slightly smaller that the magnetization at saturation in the perpendicular configuration. Hence, the coercive field for the parallel configuration will be smaller than in the perpendicular configuration. Both the dependence of the magnetization at saturation (Fig. 5) and coercive field (Fig. 7) on the spinning frequency is at variance with this prediction. The annealing seems to enhance this anisotropy supporting the hypothesis that the self-assembly features of the matrix are responsible for this anisotropy. Nevertheless, at large spinning frequency the matrix is too stresses so that a relaxation towards a self-organized morphology is no longer possible.

5. Conclusions

Magnetic measurements on SBS–BaFe nanocomposites are reported. The hysteresis loops revealed a complex dependence of the hysteresis loop parameters on the spinning frequency. The analysis of experimental data indicated that a main contribution is due to the fact that higher spinning frequencies remove from the nanocomposite film bulkier nanoparticles, displacing the distribution to smaller sizes and accordingly to superparamagnetic particles. The presence of superparamagnetic particles was suggested from the analysis of the derivative of the hysteresis loop. The possibility of self-organization processes is supported by the difference in the coercive field in parallel and perpendicular configuration on the spinning frequency, probably in competition with a curling nucleation mode.

This preliminary study revealed that the spinning is susceptible to distort the self-assembly features of such block copolymers, if magnetic nanoparticles are added to the solution. The failure to significantly improve the self-organization by thermal heating may be assigned to the thickness of our deposited films. It is known that the self-assembly of these films is destroyed as the film thickness is increased. To align thicker films, poling procedures are frequently used. The weak self-assembly process noticed in pristine composite films reflects the effect of spinning and solvent evaporation. Spinning adds an additional force, acting on the polymeric matrix through nanoparticles. This is able to distort the self-assembly procedure. Chloroform, although is a very good solvent has a high evaporation rate; accordingly the macromolecular chains have no sufficient time to reach the equilibrium (self organized) state. Further studies are required to obtain a controlled distribution of magnetic nano particles in block copolymers. Reducing the spinning frequency, the solvent evaporation rate, and the film thickness would greatly improve the local morphology, resulting in an enhanced magnetic anisotropy. A narrower size distribution of magnetic particles is also important. Nevertheless, these preliminary results are encouraging, proving that the preferential distribution of magnetic nanoparticles in self organized polymeric matrices is possible.

Acknowledgements

This work has been possible due to the support of the University of New Orleans Research Enhancement Fund, of the Indiana University Cyclotron Facility, and of Center for Materials Research and Analysis, Lincoln, Nebraska.

References

[1] Anantharaman MR, Malini KA, Sindhu S, Mohammed EM, Date SK, Kulkarni SD, Joy PA, Kurian P. Tailoring magnetic and dielectric properties of rubber ferrite composites containing mixed ferrites. Bull. Mater. Sci. 2001;24(6):623–31.

[2] Edmonds KW, Binns C, Baker SH, Maher MJ, Thornton SC, Tjernberg O, Brookes NB. Magnetism of exposed and Co-capped Fe nanoparticles. J. Magn. Magn. Mater. 2000;220:25–30.

[3] Ezzir A, Dormann JL, Kachkachi H, Nogues M, Godinho M, Tronc E, Jolivet JP. Superparamagnetic susceptibility of a nanoparticle assembly: application of the Onsager model. J. Magn. Magn. Mater. 1999; 196/197:37–9.

[4] Fang HC, Yang Z, Ong CK, Li Y, Wang CS. Preparation and magnetic properties of (Zn–Sn) substituted barium hexaferrite nanoparticles for magnetic recording. J. Magn. Magn. Mater. 1998;187:129–35.

[5] Fiorani D, Dormann JL, Cherkaoui R, Tronc E, Lucari F, Orazio F, Spinu L, Nogues M, Garcia A, Testa AM. Collective magnetic state in nanoparticles systems. J. Magn. Magn. Mater. 1999;196/197: 143–7.

[6] Kodama RH. Magnetic nanoparticles. J. Magn. Magn. Mater. 1999; 200:359–72.

[7] Jonsson P, Jonsson T, Garcia-Palacios JL, Svedlindh P. Nonlinear dynamic susceptibilities of interacting and noninteracting magnetic nanoparticles. J. Magn. Magn. Mater. 2000;222:219–26.

[8] Skomski R, Liu JP, Sellmyer DJ. Quasicoherent nucleation mode in two-phase nanomagnets. Phys. Rev. B 1999;60(10):7359–65.

[9] Hamley I. The Physics of Block Copolymers. Oxford Science Publications, Oxford: Oxford University Press; 1998.